Chapter 41
Health Risk Assessment of a Floating Village Based on a Three-Dimensional Hydraulic Model

Takashi Nakamura[1#], Toru Watanabe[2], Akino Kuwagaki[1]

[1]Toyko Institute of Technology, Japan
[2]Yamagata University, Japan

[#]Corresponding author: tnakamur@tse.ens.titech.ac.jp

Abstract The transport of *Escherichia coli* (an indicator of fecal contamination) from the floating houses in Chhnok Trou was modeled using a three-dimensional hydraulic model. The model allows us to simulate *E. coli* distribution and identify where and when lake water is contaminated. The simulation also revealed that the temporal–spatial distribution of *E. coli* concentration is strongly influenced by water velocity. Then, we applied quantitative microbial risk assessment to the simulated *E. coli* distribution to estimate the probability of disease caused by pathogenic *E. coli* in the village. The estimated mean probability of disease was 0.235 over three months in the dry season, whereas the probability ranged widely from 0 to 0.997 in the floating village. This approach visualizes the distribution of health risk in the floating village and helps us determine appropriate countermeasures based on the quantitative comparison of the efficacy of possible options.

41.1 Hydraulic model for health risk assessment

As introduced in Chapters 15–17, numerical hydraulic models can provide detailed information on the water current. The utilization of such information enables us to grasp the transport properties of various substances dissolved/suspended in a water body. Especially, as the hydraulic simulation describes the spatial profile of the current speed and direction, it has the advantage of the quantitative projection of temporal and spatial distributions of substances transported from nonuniform sources (e.g., toxic chemical compounds from factory sewage drains, pathogens from outfalls of wastewater, and heavy metal seepage from waste dumpsites). Among the various

applications, a risk assessment of waterborne infectious diseases seems to be one of the most important utilizations of the hydraulic simulation. In tropical Asia, particularly in rural areas, drainage and sewage systems are still under planning or construction and insufficient sanitation is commonly found. Such insufficient sanitation and extreme precipitation associated with the monsoon cause pathogen contamination of ambient water and consequently increase the risk of waterborne infectious diseases, such as diarrhea. The mortality rate among children under 5 years of age has a strong correlation with the insufficiency of the sanitation system (Cheng et al., 2012; Headey and Palloni, 2019). Although the rate has been declining significantly since 2010, it is still relatively high in some countries of tropical Asia, for example, Cambodia 2.8%, Bangladesh 3.0%, Lao 4.7% (WHO, 2020).

Hashimoto et al. (2014) simulated the flooding at Dhaka city in Bangladesh with a two-dimensional (2D) hydraulic model. By comparing their results with questionnaires on children's diarrhea, they concluded that morbidity was probably higher in areas with a maximum flooding depth of 0.7–1.2 m than in areas with a maximum flooding depth of 0.1–0.2 m. Kazama et al. (2012) estimated a spatial distribution of disease risk at Phnom Penh city in Cambodia with a 2D integrated hydraulic model. From a spatial distribution of coliform bacteria advected with a hydraulic model, the probability of waterborne diseases was evaluated quantitatively by using a dose–response model. As a result, it was unveiled that the location of the high-risk area is changed by the flooding magnitude. As stated above, 2D hydraulic simulations are useful in assessing the disease risk by shallow floodwater, in which the pathogen concentration tends to be uniformly distributed in the vertical direction.

On the other hand, three-dimensional (3D) hydraulic simulation enables us to conduct risk assessments in a water environment where the vertical distribution of pathogens is crucial. Hoyer et al. (2015) applied a 3D hydraulic model to a large alpine lake in USA and simulated the transport of human waterborne pathogens from a recreational beach to drinking water intakes. Their model enabled the simulation of a vertical distribution of pathogens explicitly considering the vertical dispersion caused by a thermal stratification and selective degradation of pathogens by ultraviolet (UV) irradiation in the surface layer. The floating village tends to be located where the topography changes in a small area, such as a small meandering channel and the river mouth of tributaries. Therefore, a 3D hydraulic model is expected to be suitable for the simulation of flow that must have a complex 3D profile and change locally in the village.

41.2 Sanitation in floating villages

Tonle Sap Lake (TSL) contains approximately 90 floating villages. At most houses in the villages, residents use the lake water around the house for various purposes: drinking, cooking, bathing, washing, cleaning, and so on, as described in Chapter 40. Generally, a toilet in these villages is just a hole in the floor without a septic tank, although more than half of the households in water-based villages have a toilet, according to the data reported in Chapter 40. As excreta are dumped directly into lake water underneath the house without any treatment, the floating villages face a situation in which the residents can be infected easily by waterborne diseases by drinking/touching the unsafe lake water contaminated with fecal pathogens. According to Chapter 40, almost all the adults living in the floating village have experienced diarrhea at least once a year, and 18.8% of them have had severe diarrhea. Besides diarrhea, it has been suggested that a few people suffer from other waterborne diseases, such as parasitic infections and infectious gastroenteritis that spread through the lake water (Merali et al., 2014). To reduce the infection of waterborne diseases, it is important that the people gain awareness of these risks and change their behavior. A map of the disease risk in the village promises to be one of the most impressive materials to raise the people's awareness, because the map clearly shows the location of the unsafe water and how risky it is. In some previous studies, these kinds of disease risk maps were generated by using 2D hydraulic simulation models (Amano et al., 2012; Kazama et al., 2012). However, the maps were made to show the spatial distribution of the risk at a regional scale (up to 100 km); no past study has assessed a risk map at the village scale by solving a local structure of water flow with a 3D hydraulic model. Therefore, this chapter describes the application of the quantitative risk assessment of waterborne infectious diseases to one of the major floating villages, Chhnok Trou, to demonstrate the usefulness of a 3D hydraulic model and a risk map.

41.3 Simulation of *E. coli* transport

As feces is the main source of waterborne pathogens, *Escherichia coli* bacteria, which are found commonly in the intestines of people and animals, is normally used as an indicator to represent the extent of fecal pollution. In the quantitative microbial risk assessment (QMRA), the disease probability is evaluated by a dose–response model with the concentration of *E. coli* (Haas et al., 1999; WHO, 2016). In the present work, the temporal and spatial distributions of the *E. coli* concentration, which is assumed to be dumped from each floating house, is assessed by solving the following advection–diffusion equation:

$$\frac{\partial C}{\partial t} + u\frac{\partial C}{\partial x} + v\frac{\partial C}{\partial y} + w\frac{\partial C}{\partial z} =$$

$$\frac{\partial}{\partial x}\left(\frac{K_H}{\sigma_C}\frac{\partial C}{\partial x}\right) + \frac{\partial}{\partial y}\left(\frac{K_H}{\sigma_C}\frac{\partial C}{\partial y}\right) + \frac{\partial}{\partial z}\left(\frac{K_V}{\sigma_C}\frac{\partial C}{\partial z}\right) - \frac{C}{\tau_C}, \quad (41.1)$$

where $C(t,x,y,z)$ is the concentration of *E. coli*, K_H and K_V are kinematic viscosity in the horizontal and vertical directions, respectively, and σ_C is a Schmidt number for the diffusion process of *E. coli*. In this work, we set $\sigma_C = 1$. τ_C as the lifetime in which *E. coli* is reduced to e^{-1} times of the initial population. According to the field experiment conducted in TSL (Tan et al., 2017), τ_C was set at 10 hours.

The locations of all houses (totally 1,362 houses) in the Chhnok Trou floating village were obtained from a satellite image in Google Earth (captured on January 1, 2017). The emission of *E. coli* from houses to lake water was then modeled as follows: *E. coli* is excreted from each house every morning; the time of excretion is distributed randomly from 4 to 8 AM; the weight of feces excreted by each person is about 105 g (Tanaka et al., 1975); the *E. coli* concentration in feces is 10^9 colony-forming units (CFU)/g (Ervin et al. 2013); and there were five family members in each house (NIS, 2002). As the emission of *E. coli* and water withdrawal are both done at the water surface, the *E. coli* concentration is expected to have a nonuniform vertical distribution. Therefore, a 3D model, the Tokyo Institute of Technology–WAter Reservoir Model (TITech-WARM), was applied. The temporal–spatial change of *E. coli* concentration was projected by solving Eq. (41.1) along with hydraulic equations (see Chapter 17 for details).

The 3D simulation was conducted for 1 week in the dry season (from March 3 to 10, 2018). Figure. 41.1 shows the calculated daily change in the *E. coli* concentration at the water surface on March 10, 2018. The calculated result showed that the reduction rate of the *E. coli* concentration depends strongly on the topographic condition. A spatial distribution of the flow speed is shown in Figure. 17.4 in Chapter 17. As shown in Figure. 41.2, in a channel where many houses are located and the water flow is relatively rapid (St. U), the *E. coli* concentration reduces to the WHO standard for the drinking water ($C < 1$ CFU/100 ml) before noon. On the other hand, in a stagnant water area, such as a clogged canal (St. P), the concentration remains 1,000 times higher than the WHO standard throughout the day. This difference in the reduction rate suggests that the disease risk of pathogenic *E. coli* is possibly reduced by selecting an appropriate time and location to collect the lake water for drinking (e.g., in the evening, upstream of a central area where the houses are not crowded, and the water flow is relatively fast).

As exemplified in this simulation, in general, the simulation of the *E. coli* with the hydraulic model can produce persuasive materials to support

environmental awareness activities and encourage the residents to change their behavior to access safe water even though the floating villages cause fecal pollution. The field observations of *E. coli* were made on March 14 and 15, 2019. In Figure. 41.2, the observational data are shown in black and blue symbols. Although it is not an accurate verification because the year is different from the

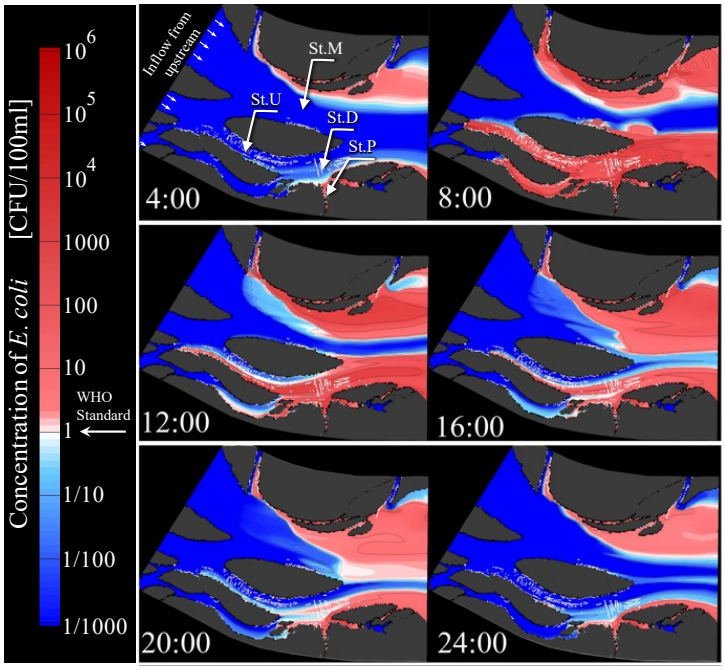

Figure. 41.1 Diurnal change of the *E coli*. concentration calculated by the 3D transport simulation on March 10, 2018. The concentration at the water surface is shown, whereas a 3D profile of the concentration was calculated in the simulation.

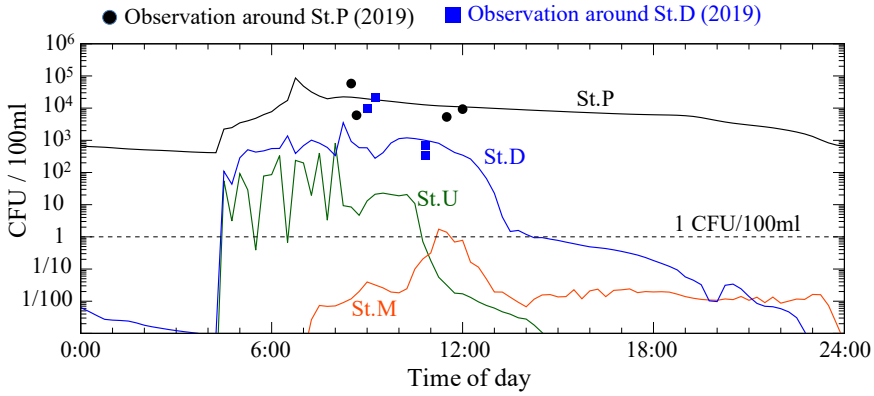

Figure. 41.2 Temporal change of the calculated *E. coli* concentration at the water surface on March 10, 2018. The locations of observational points (St. P, St. D, St. U, and St. M) are shown in Figure. 41.1. Black circles and blue squares represent data observed on May 14 and 15, 2019, respectively.

the simulation, the observed data agree with the calculation and the simulation seems to calculate reasonable *E. coli* transport to a certain extent.

41.4 Quantitative microbial risk assessment (QMRA)

Based on the simulated 3D flow field, QMRA was applied to the calculated spatial distribution of *E. coli*. To estimate the probability of waterborne diseases (diarrhea, fever, gastroenteritis) caused by pathogenic *E. coli*, the following dose–response model of the beta-Poisson type was used (Hoang et al., 2011):

$$P(D) = 1 - \left[1 + \frac{D}{N_{50}}(2^{1/\alpha} - 1)\right]^{-\alpha}, \qquad (41.2)$$

where $P(D)$ is the probability of disease after a person ingests D cells of *E. coli* in a day. As parameters, we used $\alpha = 0.1778$ and $N_{50} = 8.6 \times 10^7$. The model utilized is designed to evaluate the disease risk of pathogenic *E. coli*. As a non-pathogenic strain is counted in the *E. coli* concentration calculated in the transport simulation, the risk evaluated using the above model is expected to be larger than the actual probability of disease. From the $P(D)$, we can estimate the probability of disease per d days P_d:

$$P_d = 1 - \left[1 - P(D)\right]^d, \quad (41.3)$$

In this work, we assumed that the people ingest *E. coli* by drinking water, by accidental ingestion, and through polluted vegetables.

$$D = D_{drink} + D_{accident} + D_{vegetable} \qquad \text{[CFU/day]}, \qquad (41.4)$$

These three assumed ingestions were quantified as follows.

Ingestion by drinking water (D_{drink})

Although some people in the floating village use bottled water for drinking, the questionnaire survey (**Chapter 40**) showed that half of the people in the village use the lake water for drinking purposes, and about 30% of the people drink it without any water treatment. To assess the risk faced by the people drinking such untreated water, we estimated the dose by drinking (D_{drink}) based on the *E. coli* concentration calculated using the 3D hydraulic model:

$$D_{drink} = L_{drink} \times \bar{C}_{day}, \qquad (41.5)$$

where L_{drink} is the volume of water that an adult drinks in a day, and we assumed $L_{drink} = 2.6$ L/day (NHMRC and NZ MoH, 2016). Although the *E. coli* concentration changes over time, as shown in Figure. 41.1, we used the average daily *E. coli* concentration at the water surface $\bar{C}_{day}$ (Figure. 41.3a) because of the lack of detailed information on when the people withdraw the lake water.

Ingestion by accident ($D_{accident}$)

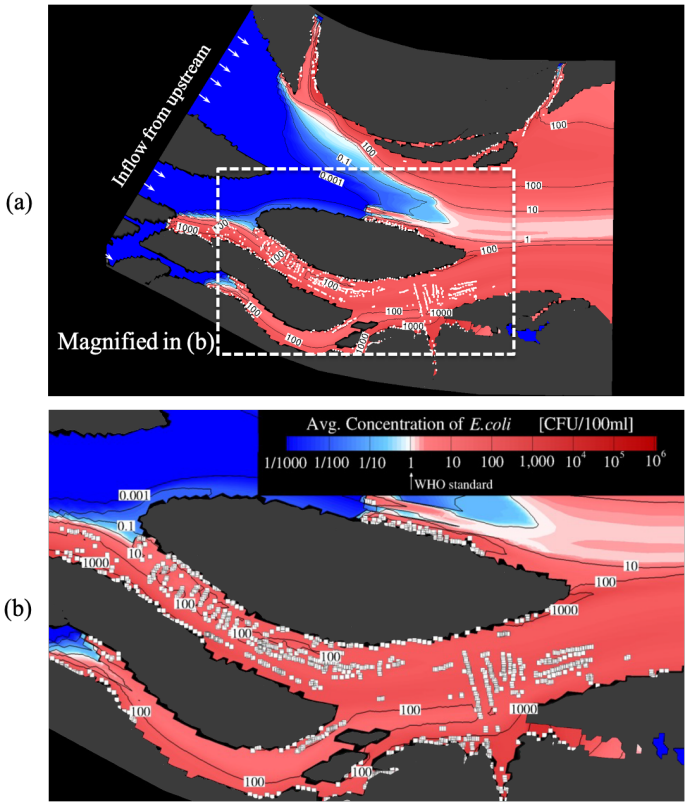

Figure. 41.3 Distribution of the daily average *E. coli* concentration at the water surface in (a) a whole simulated area and (b) the central area of Chhnok Trou village. White squares represent locations of houses.

As to causes of accidental ingestion of the lake water, we assumed they both occurred from swimming and bathing in the lake.

$$D_{accident} = L_{swimming} \times \bar{C}_{day} + L_{bathing} \times \bar{C}_{day}, \quad (41.6)$$

By assuming that the active time for swimming and bathing are $T_{swimming} = 10$ min and $T_{bathing} = 17$ min, respectively, the volumes of water ingestion were evaluated as follows:

$$L_{swimming} = T_{swimming} \times U_{swimming}, \quad (41.7)$$

$$L_{bathing} = T_{bathing} \times U_{bathing}, \quad (41.8)$$

where $U_{swimming}$ and $U_{bathing}$ are the volume of ingestion per unit time and were set to 10 and 50 ml/hour, respectively, following Hoang et al. (2011).

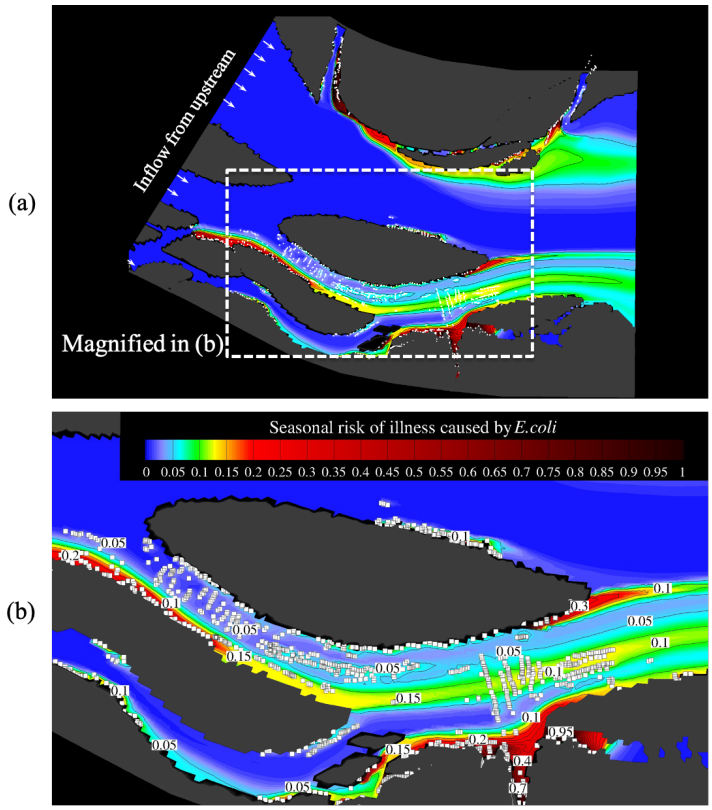

Figure. 41.4 Distribution of disease probability over three months. In each panel, the location of each floating house is shown as a white square.

Adhesion to vegetables ($D_{vegetable}$)

In Cambodia, raw vegetables are commonly consumed. Washing the vegetables with contaminated water probably causes adhesion of the waterborne pathogens to vegetables. By referring to the QMRA for Hue city in Vietnam (Hoang et al., 2011), we assumed that an adult person eats 4.1 g of raw vegetables per day and five cells of *E. coli* adhere to 1 g of vegetables.

$$D_{vegetable} = 4.1[\mathrm{g/day}] \times 5[\mathrm{CFU/g}] = 20.5[\mathrm{CFU/day}] \quad (41.9)$$

As a result of QMRA, the spatial distribution of the evaluated probability of disease over 3 months (P_{93}) is illustrated in Figure. 41.4. As shown in Figure. 41.4b, the disease risk clearly varies by location. Although the probability is less than 0.05 at the center of each water channel where water flows rapidly, the probability reaches a maximum of about 10 times more at the shallow area along the shoreline where the water is stagnant. Figure. 41.5 shows the frequency

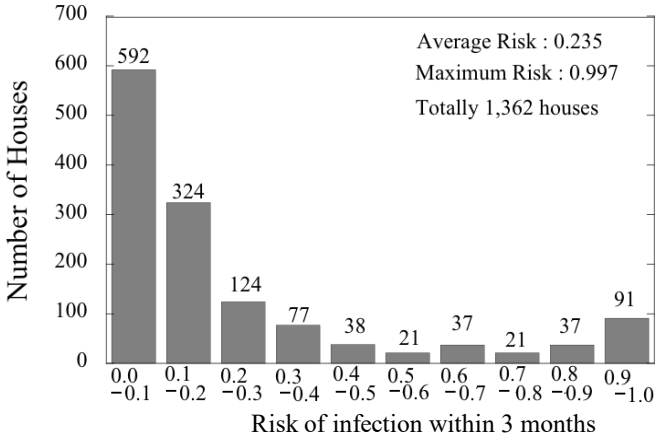

Fig. 41.5 Number of houses for each range of disease probability over three months.

distribution of disease probability of the floating houses. The average disease probability was 0.235. This average probability was converted to 0.46 of a 7-month probability by applying Eq. (41.3) again. Although this value is less than 0.8 reported by In et al. (2017), based on a questionaries' survey, the order of magnitude of the probability is agreeable. As QMRA generally estimates the probabilities under many assumptions, we cannot expect that the estimated probabilities match the actual situation exactly. Therefore, instead of using the probabilities calculated by QMRA as they are, we should utilize QMRA to assess the effectiveness and benefits of the policies (WHO, 2016) by comparing the possibilities, as explained below.

Even in the same village, the probability ranged widely from 0 to 0.997. Among all the houses in Chhnok Trou (1,362 houses), 43.5% of houses (592 houses) are located where the disease risk is lower than 0.1. On the other hand, 32.7% of houses (446 houses) are located where the disease probability is higher than 0.2, meaning that at least one of five family members is infected in 3 months. This result suggests that the possibility of the disease risk can be reduced to less than 0.2 by simply relocating 32.7% houses from the high-risk area to the low-risk area. According to our trial calculation on the assumption that the disease risk of the relocated houses is reduced to $P_{93} = 0.2$, the average disease probability was reduced from 0.235 to 0.121. Assuming that there are five family members per house, this reduction means that the number of patients is reduced from 1,600 to 824 persons in three months.

As shown in this case study, the approach integrating the hydraulic model and QMRA visualizes the distribution of healthy risk in a floating village. Besides the floating village, the approach can be applied to various water areas and help us determine appropriate countermeasures based on the quantitative

comparison of efficacy of possible options (e.g., encouraging hand washing with soap and simple purification of water before drinking, such as coagulation sedimentation). Moreover, the impacts of global warming and dam construction on health risks could be assessed if hydraulic conditions in the future could be assumed as computational conditions used in the hydraulic model.

41.5 Key points

1. The spread of *E. coli* that is dumped into the lake water from floating houses was simulated for Chhnok Trou floating village. The transport of *E. coli* because of the water flow was modeled with an advection–diffusion equation using a 3D hydraulic model, the Tokyo Institute of Technology–WAter Reservoir Model (TITech-WARM).
2. The simulation of Chhnok Trou clearly showed the temporal and spatial change of *E. coli* distribution in the village. From the results, we can read the spatial and temporal distributions of the unsafe contaminated water. The simulation provides rather impressive results, which help with environmental awareness activities and encourage the residents to change their behavior to prevent water-borne diseases.
3. From the simulated distribution of *E. coli*, the disease probability was evaluated using QMRA. Besides using QMRA to visualize the current health risks, it was confirmed that QMRA can help us to take appropriate measures by evaluating the efficacy of measures quantitatively.

References and further reading

Amano, A., Sakuma, T. et al. (2012) Evaluation of diarrhea disease risk attributed to inundation water use on a local scale in Cambodia using hydrological model simulations, River System 20:185-196.

Australian National Health and Medical Research Council and the New Zealand Ministry of Health (NHMRC and NZ MoH) (2016) Nutrient Reference Values, Retrieved February 4th, 2021 from https://www.nrv.gov.au/.

Cheng, J. J., Schuster-Wallace, C. J. et al. (2012) An ecological quantification of the relationships between water, sanitation and infant, child, and maternal mortality, Environmental Health 11 DOI:10.1186/1476-069X-11-4.

Ervin, J. S., Russell, T. L. et al. (2013) Characterization of fecal concentrations in human and other animal sources by physical, culture-based, and quantitative real-time PCR methods, Water Research 47: 6873-6882.

Haas, C. N., Rose, J. B. et al. (1999) Quantitative microbial risk assessment. John Wiley & Sons, Inc. ISBN: 978-1-118-14529-6.

Hashimoto, M., Suetsugi, T. et al. (2014) Assessing the relationship between inundation and diarrhoeal cases by flood simulations in low-income communities of Dhaka City, Bangladesh. Hydrological Research Letters 8:96-102.

Headey, D., Palloni, G. (2019) Water, sanitation, and child health: evidence from subnational panel data in 59 countries. Demography 56: 729-752.

Hoang, T. M., Watanabe, T. et al. (2011) Quantitative risk assessment of infectious diseases caused by waterborne *Escherichia coli* during floods in cities of developing countries, Journal of Japan Society on Water Environment 34: 153-156.

Hoyer, A. B., Schladow, S. G. et al. (2015) A hydrodynamics-based approach to evaluating the risk of waterborne pathogens entering drinking water intakes in an large, stratified lake. Water Research 83: 227-236.

Kazama, S., Aizawa, T. et al. (2012) A quantitative risk assessment of waterborne infectious disease in the inundation area of a tropical monsoon region. Sustainability Science 7:45-54.

Merali, H. S., Morgan, J. F. et al. (2014) The lake clinic - providing primary care to isolated floating villages on the Tonle Sap Lake, Cambodia. Rural and Remote Health 14: 2612.

National Institute of Statistics (NIS) (2002) General population census of Cambodia 1998, final census results (2nd edition), Ministry of Planning : 88.

Tan, R., Chanto MCT. Et al. (2017) Survival of Escherichia coli K12 in Tonle Sap Lake and Tonle Sap Water by using dialysis membrane as a supporter, Proceeding of the 2nd international symposium on conservation and management of tropical lakes: 133-139.

Tanaka, Y., Hayashida, S. et al. (1975) The relationship of the feces protein particles to rice protein bodiest, Agricultural and Biological Chemistry 39: 515- 518.

WHO (2016) Quantitative microbial risk assessment: application for water safety management. https://apps.who.int/iris/handle/10665/246195 (Accessed in 17th June, 2021).

WHO (2020) World Health Statistics 2020, https://apps.who.int/iris/bitstream/handle/10665/332070/9789240005105-eng.pdf (Accessed in 27th Dec, 2020).